Addressing Mechanical and Electrochemical Aging of Cylindrical LFP Battery Cells by Laser Structuring of Electrodes

Yannic Sterzl
Institute for Applied Materials - Applied Materials Physics
Karlsruhe Institute of Technology
Karlsruhe, Germany
yannic.sterzl@kit.edu

Shizhou Xiao
EdgeWave GmbH
Würselen, Germany
xiao@edgewave.com

Martin Pulst
EAS Batteries GmbH
Nordhausen, Germany
martin.pulst@eas-batteries.com

Wilhelm Pfleging
Institute for Applied Materials - Applied Materials Physics
Karlsruhe Institute of Technology
Karlsruhe, Germany
wilhelm.pfleging@kit.edu

***Abstract*— First results for the implementation of ultrafast laser structured thick-film lithium iron phosphate (LFP) electrodes in cylindrical battery cells are presented, with a special focus on laser structuring without thermal modification of the active material and the winding quality of thick-film electrodes. It was shown in half-cell measurements that minor thermal modifications did not result in a reduction in specific capacity of laser structured electrodes. Cells with structured electrodes had a higher rate capability at discharge C-rates greater than 1C compared to cells with unstructured electrodes. Furthermore, line structured electrodes with a structure pitch of 300 µm showed no visible damage of the electrode coating after winding at a radius of 3 mm, whereby the unstructured reference electrodes showed visible crack formation and delamination from the current collector after winding at a radius of 5 mm.**

Keywords — 3D battery, electrode architecture, LFP, laser structuring, cylindrical cells, winding quality

I. INTRODUCTION

Increasing electrification poses new challenges for the development of advanced lithium-ion batteries in terms of fast-charging capability, lifetime, safety, and manufacturing costs [1]. For this reason, innovative electrode architectures are being investigated for lithium-ion batteries that enable high energy and power density at cell level. This involves combining different active materials, either as a mixture or as a multilayer structure, or reducing the effective tortuosity of the electrode through structuring [2-5]. Electrode structuring can be performed by additive manufacturing, mechanical ablation, or laser ablation [5-7]. The focus of this work is on laser structuring, due to the easy integration of the process into industrial production and the flexibility in the choice of the structure pattern to be realized, as the pattern has a great influence on the later electrochemical performance of the cell [8, 9]. This is mainly due to the significantly shortened lithium-ion transport distances in the generated 3D electrodes and the strongly accelerated and overall homogenized electrolyte wetting and re-wetting of electrodes as a result of capillary effects [6, 10]. However, the advantages of implementing 3D electrodes must also be assessed with regard to the cell format. The advantages of implementing laser structured electrodes have been demonstrated in coin cells, single-layer lab pouch cells, as well as in large-format multi-layered pouch cells in terms of increased cycle life and rate capability [4, 11, 12]. For cylindrical cells, structuring the electrodes not only offers improvements in terms of wetting with liquid electrolyte and lithium-ion diffusion kinetics, but also the possibility of ensuring the mechanical integrity of the electrodes [13]. The curvature of the electrodes is highest in the center of the jelly roll, which can lead to delamination of the coating and changes in the porosity of the coating in the case of thick-film, i.e., high mass loaded electrodes [13]. The implementation of line structures vertically to the winding direction and the associated free space could help to avoid film cracking and film delamination during winding and ensure a more homogeneous porosity in the electrode. The concept is shown schematically in Fig. 1. The potential advantages in terms of structuring are particularly pronounced for electrodes with a high coating thickness, such as those found in high-energy cells [14]. Particular attention should be paid to electrodes with lithium iron phosphate (LFP) as the active material. Cells with LFP as the cathode active material are gaining an increasing market share due to their lower costs compared to cells with NCA or NMC as the cathode active material [14]. One disadvantage is the low achievable energy densities of cells with LFP as cathode material due its low specific capacity of about 150 mAh g^{-1} [15]. The low specific capacity of LFP compared to nickel-rich NMC leads to electrodes with high coating thicknesses, which in turn causes the already mentioned problems in processability and electrochemical properties and are therefore the subject of current research with regard to laser structuring [14, 16, 17]. The material modification of LFP described in literature, that

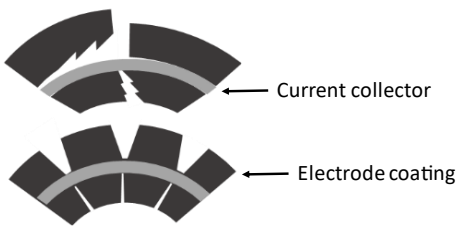

Fig. 1. Schematical illustration of possible advantages of line structured electrodes (cross sectional view) with regard to the mechanical integrity of wound electrodes.

occurs during laser structuring with laser pulse durations in the nanosecond (ns) regime, must be counteracted by using ultrashort pulses (USP) in the femtosecond (fs) regime and suitable structuring parameters [16].

The work presented here focuses on the laser structuring of LFP thick-film electrodes. Suitable process windows for laser structuring are defined in order to avoid thermal modifications of the active material, and the winding quality is demonstrated on cross-section samples with different winding radii. The greater rate capability of cells with structured electrodes compared to cells with unstructured electrodes is demonstrated in half-cell analyses.

II. Experimental

A. Laser structuring and electrode characterization

Commercial double-side coated LFP electrodes (EAS Batteries GmbH, Nordhausen, Germany) with an areal capacity of 3.16 mAh cm^{-2} and a single-sided coating thickness of 125 µm were laser structured with a high power and high repetition rate laser system (FX600, EdgeWave GmbH, Würselen, Germany), operating at a wavelength of 1030 nm, a pulse width of 600 fs and a max. laser average power of 300 W. The LFP electrodes were structured at repetition rates of 150 kHz and 1.5 MHz and pulse peak fluences between 7 J cm^{-2} and 33 J cm^{-2} with an increasing number of laser scan passes. The pulse overlap was kept constant, and thus the scanning speed was fixed at 2 m s^{-1} at 150 kHz and 20 m s^{-1} at 1.5 MHz. The ablation depth of the structured electrodes were examined via focus variation using a digital microscope (VHX7000, KEYENCE, Osaka, Japan). The measurement range was limited to an ablation depth of 60 µm, as sufficient illumination of the channels and thus reliable measurement could no longer be guaranteed at ablation depths greater than 60 µm. In addition, the laser structured electrodes were examined on a scanning electron microscope (SEM, Phenom Pro, Thermo Fischer Scientific, Waltham, MA, USA) to characterize the impact of the repetition rate and the pulse peak fluence on the formation of thermally-driven modifications on the LFP active material. Structured electrodes with line pattern and unstructured electrodes were winded onto additively manufactured cores with diameters of 6 mm and 10 mm and characterized by cross-section analyses using a light microscope (Reicher-Jung MeF3, Leica Microsystems, Wetzlar, Germany) to determine differences in winding quality. The electrodes for the winding test were laser structured on both sides at an average laser power of 60 W, a scanning speed of 20 m s^{-1} and 21 laser scan passes. The line structure pitch was varied between 300 µm and 600 µm.

B. Electrochemical characterization

For the electrochemical characterization, the coating on one side of the double-sided coated electrodes was removed via laser ablation. Electrodes with a diameter of 12 mm were laser cut and subsequently dried in a vacuum oven at 100 °C for 24 h to remove excess moisture. Half-cells in CR2032 coin cell format were assembled in an argon-filled glove box (LAB master pro sp, M. Braun Intergas-Systeme GmbH, Garching, Germany) with $H_2O < 0.1$ ppm and $O_2 < 0.1$ ppm. As electrolyte, 1M $LiPF_6$ salt in a solvent mixture of ethylene carbonate, ethyl methyl carbonate, and dimethhyl carbonate with 2 wt.% VC additive was used. Each half-cell was constructed of one electrode, 160 µL of electrolyte, a 25 µm polypropylene (PP) separator, a 600 µm thick lithium chip and were stored for 20 h at 20 °C prior to further electrochemical analyses to ensure a homogeneous wetting of the electrodes and separator with liquid electrolyte. Galvanostatic cycling with potential limitations (GCPL) was performed using a battery cycler (BT 2000, Arbin Instruments, College Station, TX, USA). The formation of the half-cells was performed in a voltage window of 2.5–3.8 V following a constant current (CC) constant voltage (CV) protocol at a charging and discharging current rate (C-rate) of 0.025C and a cut-off current in the charging CV phase of 0.0125C. The term "C-rate" is a measure of the rate at which a battery is being discharged in relation to the maximum capacity of the battery. Three conditioning cycles at 0.2C charging and discharging were preformed after the formation cycle. The rate capability analyses subsequently to the formation and conditioning cycles consisted of CCCV charging at 0.5C (cut-off CV-phase 0.25C) and CC discharging with increasing discharging rates from 0.2C to 15C.

III. Results and Discussion

A. Laser structuring

A thermally-induced modification of the electrode material by laser ablation should be avoided or suppressed due to the possible negative impacts on the electrochemical performances, such as a lower specific capacity and a reduced cell lifetime. It has been found that laser processing of LFP requires narrow process windows and special process optimization to avoid or limit thermal modification of the active material, especially for laser structuring by using pulse widths in the nanosecond (ns) regime, high laser power or repetition rates greater 500 kHz [16, 18]. Structuring at high repetition rates, however, has advantages in the achievable processing speed, as the scanning speed can also be increased with increasing repetition rate while maintaining the same pulse overlap [19]. Therefore, a trade-off must be found between possible thermal modifications and structuring parameters such as repetition rate and pulse peak fluence. In Fig. 2 the effects of structuring with various pulse peak fluences and repetition rates on the thermal modification of LFP electrodes in top view SEM analysis are shown. The structuring at a repetition rate of 1.5 MHz and a pulse peak fluence of 33 J cm^{-2} leads to a thermally-driven material modification along the sidewalls of the laser generated grooves (Fig. 2a). Material modifications due to laser

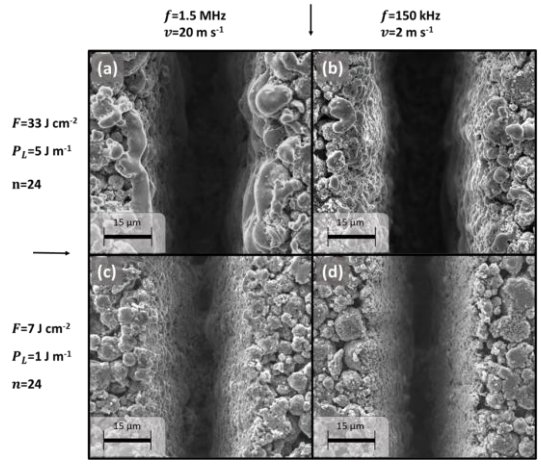

Fig. 2. Top view SEM images of laser structured LFP electrodes structured at 1.5 MHz, 33 J cm-2 and 20 m s-1 (a), 150 kHz, 33 J cm-2 and 2 m s-1 (b), 1.5 MHz, 7 J cm-2 and 20 m s-1 (c) and 150 kHz, 7 J cm-2 and 2 m s-1 (d), and with 24 laser scan passes.

structuring could not be observed in the SEM analysis with a reduction in the pulse peak fluence to 7 J cm^{-2} (Fig. 2c), a reduction in the laser repetition rate to 150 kHz (Fig. 2b) or a combination of both (Fig. 2d). Material modifications along the groove sidewalls due to laser structuring can therefore be significantly reduced or even avoided by structuring at moderate pulse peak fluences and/or repetition rates. For the electrode laser structuring to be implemented in industrial cell manufacturing, an accurate knowledge of the ablation characteristic is important to precisely adjust the mass removal rate and groove geometry. In Fig. 3, the ablation depth as a function of the logarithmic peak fluence is shown for the ablation at 150 kHz and 1.5 MHz with six laser scan passes. The ablation depth increases with increasing peak fluence, whereby the ablation depth also depends on the laser repetition rate. A dependence of the ablation depth on the repetition rate is known for various electrode materials and may be associated with material vapor/plasma shielding effects [20]. Thus, the ablation depth achieved at a peak fluence of 26 J cm^{-2} and a repetition rate of 1.5 MHz is 33 µm and at a repetition rate of 150 kHz 40 µm. This results in an increase in the ablation depth of 21%, at the same peak fluence. However, due to the constant pulse overlap, the scanning speeds at 150 kHz with 2 m s^{-1} are 10 times lower compared to the structuring at 1.5 MHz and 20 m s^{-1}. This results in the conclusion that it would be favorable to work with high repetition rates in order to further upscale the structuring process, as the advantages of a higher scanning speed with a high repetition rate outweigh the higher ablation depth at low repetition rates.

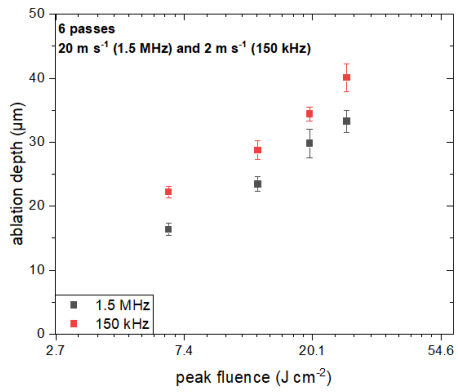

Fig. 3. Ablation depth as a funcion of pulse peak fluence at a repetition rate of 150 kHz and 1.5 MHz, constant pulse overlap, and 6 laser scan passes.

B. *Electrochemical characterization*

To characterize the impact of thermally-driven modifications by laser structuring, half-cells were manufactured with electrodes which were laser structured by parameters shown in Fig. 4b-f, with and without thermally-driven modifications as well as an unstructured reference. All studied types of electrodes reached similar specific discharge capacities at a C-rate of 0.2C of 145 mAh g^{-1}. This indicates that the identified thermally-driven modification due to laser structuring do not result in a significant loss of specific capacity of the active material. It is assumed that this is mainly due to the small amount of affected active material as well as the small thermal penetration depth. The positive influence of the structuring on the diffusion kinetics of the line-structured electrodes compared to the unstructured reference electrodes is evident at discharge with C-rates greater than 1C. In the case of discharging at 3C, a specific discharge capacity of

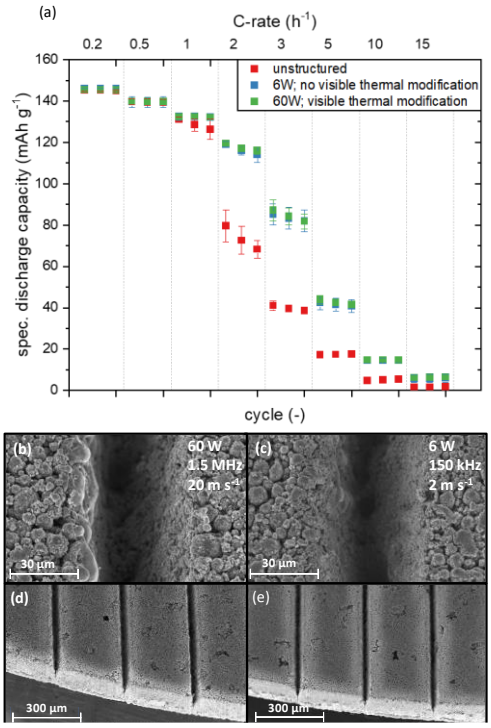

Fig. 4. Specific discharge capacity of half-cells with structured electrodes with and without visible thermal modification of the active material, and unstructured reference electrodes (a), as well as the SEM analysis of the respective structured electrodes with (b,d) and without (c,e) thermally-driven modifications.

82 mAh g^{-1} was reached for cells with structured electrodes, whereas the cells with unstructured electrodes reached a specific capacity of 39 mAh g^{-1}. A positive effect on the charge and discharge capability of cells with structured electrodes has also recently been demonstrated in several studies [21, 22].

C. *Winding quality*

One of the challenges of increasing the energy density of cylindrical cells is the limitation of the coating thickness of the electrodes that can be utilized due to mechanically-induced film defects (cracks, delamination) during winding. The introduction of line structures vertically to the winding direction can prevent damage to the coating with small winding radii, by enabling the expansion and compression of the electrode due to the free space provided by the structure. This is shown in Fig. 5 for electrodes structured on both sides with a pitch of 300 µm and 600 µm. The electrodes are structured similar to the electrodes in Fig. 4b,d. As can be seen in Fig. 5a,d, the unstructured electrodes already show the first crack formations in the coating at a winding radius of 5 mm. It was not possible to wind the unstructured electrodes with a winding radius of 3 mm due to complete coating delamination (not shown here). Structured electrodes with a pitch of 300 µm, on the other hand, can still be processed without visible film defects even at a winding radius of 3 mm (Fig. 5b,e). The structured electrodes with a structure pitch of 600 µm showed film defects in the form of layer delamination on the top of the electrode at a winding radii of 3 mm (Fig. 5c,f). Preventing damage is therefore a function of the structure pitch and must be adjusted to the respective later winding radius in the cylindrical cell. In our case, structuring with a pitch of 300 µm, which corresponds to a mass loss of less than 5 %, prevented coating damage due to winding at a radius of 3 mm.

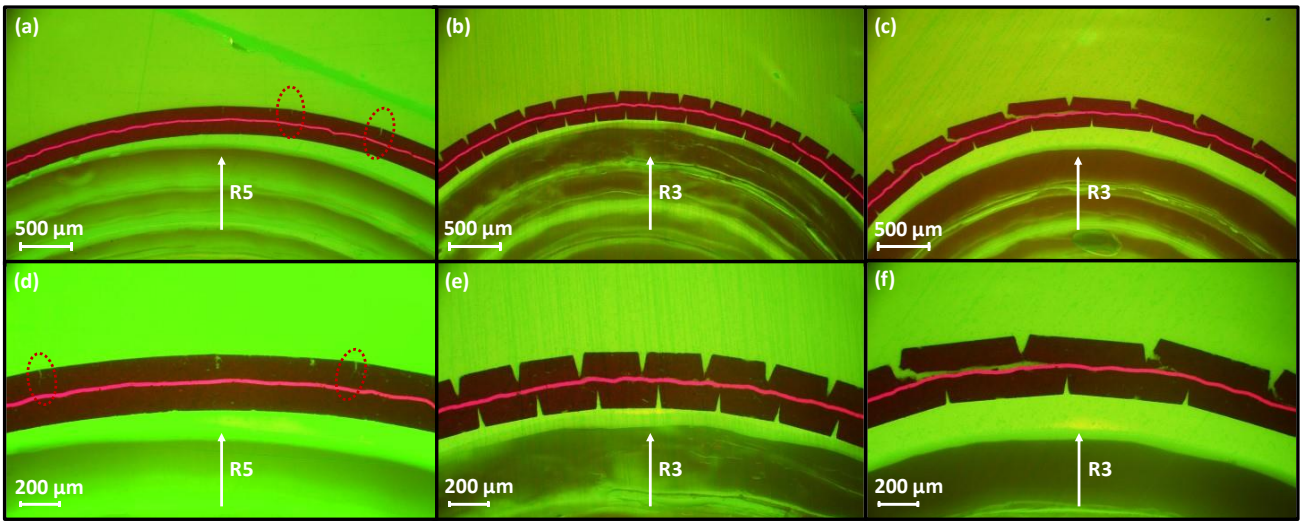

Fig. 5. Light microscope images of the cross-sections of unstructured LFP electrodes at a winding radius of 5 mm (R5) with visible crack formation (a,d), structured electrodes at a structure pitch of 300 µm and a winding radius of 3 mm (R3) without visible crack formation (b,e), and structured electrodes with a structure pitch of 600 µm and visible crack formation and film delamination (c,f).

IV. Conclusion

First results on the implementation of ultrafast laser structured thick-film LFP electrodes in cylindrical battery cells were presented. Laser and process parameters like laser fluence and repetition rate were evaluated with regard to a laser-induced modification of LFP electrodes, and the generated structures were examined by scanning electron microscopy and digital microscopy. It was shown that visible thermally-driven modifications occur on the LFP electrodes during structuring with repetition rates of 1.5 MHz and elevated peak fluences of 33 J cm^{-2}. A reduction of the pulse peak fluence to 7 J cm^{-2}, a reduction in the repetition rate to 150 kHz or a combination of both suppressed the thermally-induced modification of LFP electrodes. The influence of the repetition rate and the peak fluence on the ablation depth was also examined for LFP electrodes, and the vapor/plasma shielding effects with increasing repetition rate known from other electrode materials was also observed for LFP electrodes. In addition, the impact of low thermally-driven modifications on LFP electrodes by laser structuring was characterized electrochemically in half-cells. Electrodes structured at 60 W and 1.5 MHz showed the same specific capacity at low C-rates of 0.2C as the unstructured reference and the electrodes structured at 6 W and 150 kHz without thermally-driven modifications. Furthermore, it was demonstrated that the formation of film cracks and film delamination of LFP electrodes can be prevented at small winding radii by applying a line structure design. Thick-film electrodes, which were structured with a structure pitch of 300 µm, could be winded at a radius of 3 mm without visible film defects, while unstructured electrodes or electrodes with a structure pitch of 600 µm could not be winded without formation of cracks or film delamination. In ongoing work, the results of the coin cell analyses and the winding tests will be transferred to the assembly of cylindrical cells with optimized electrode architectures.

Acknowledgment

We are grateful to our colleagues M. Kapitz, and A. Reif for their technical and scientific support in laser processing and scanning electron microscopy. This project has received funding from the Federal Ministry of Education and Research (BMBF, High-E-Life, 03XP0495) and scientific research exchange supported by EU-L4DNANO (HORIZON, project No. 101086227).

References

[1] R. Schmuch, R. Wagner, G. Hörpel, T. Placke, and M. Winter, "Performance and cost of materials for lithium-based rechargeable automotive batteries," *Nature Energy*, vol. 3, no. 4, pp. 267-278, 2018, doi: 10.1038/s41560-018-0107-2.

[2] L. Gottschalk *et al.*, "Improving the Performance of Lithium - Ion Batteries Using a Two - Layer, Hard Carbon - Containing Silicon Anode for Use in High - Energy Electrodes," *Energy Technology*, vol. 11, no. 5, 2022, doi: 10.1002/ente.202200858.

[3] K. H. Chen *et al.*, "Enabling 6C Fast Charging of Li - Ion Batteries with Graphite/Hard Carbon Hybrid Anodes," *Advanced Energy Materials*, vol. 11, no. 5, 2020, doi: 10.1002/aenm.202003336.

[4] K.-H. Chen *et al.*, "Efficient fast-charging of lithium-ion batteries enabled by laser-patterned three-dimensional graphite anode architectures," *Journal of Power Sources*, vol. 471, 2020, doi: 10.1016/j.jpowsour.2020.228475.

[5] U. Rist, V. Falkowski, and W. Pfleging, "Electrochemical Properties of Laser-Printed Multilayer Anodes for Lithium-Ion Batteries," *Nanomaterials (Basel)*, vol. 13, no. 17, Aug 25 2023, doi: 10.3390/nano13172411.

[6] W. Pfleging, "Recent progress in laser texturing of battery materials: a review of tuning electrochemical performances, related material development, and prospects for large-scale manufacturing," *International Journal of Extreme Manufacturing*, vol. 3, no. 1, 2020, doi: 10.1088/2631-7990/abca84.

[7] J. Keilhofer *et al.*, "Mechanical Structuring of Lithium - Ion Battery Electrodes Using an Embossing Roller," *Energy Technology*, vol. 11, no. 5, 2023, doi: 10.1002/ente.202200869.

[8] L. Hille *et al.*, "Integration of laser structuring into the electrode manufacturing process chain for lithium-ion batteries," *Journal of Power Sources*, vol. 556, 2023, doi: 10.1016/j.jpowsour.2022.232478.

[9] Y. Sterzl and W. Pfleging, "Optimizing Structural Patterns for 3D Electrodes in Lithium-Ion Batteries for Enhanced Fast-Charging Capability and Reduced Lithium Plating," *Batteries*, vol. 10, no. 5, 2024, doi: 10.3390/batteries10050160.

[10] W. Pfleging and J. Pröll, "A new approach for rapid electrolyte wetting in tape cast electrodes for lithium-ion batteries," *J. Mater. Chem. A*, vol. 2, no. 36, pp. 14918-14926, 2014, doi: 10.1039/c4ta02353f.

[11] A. Meyer, P. Zhu, A. Smith, and W. Pfleging, "Gaining a New Technological Readiness Level for Laser-Structured Electrodes in High-Capacity Lithium-Ion Pouch Cells," *Batteries*, vol. 9, no. 11, 2023, doi: 10.3390/batteries9110548.

[12] J. B. Habedank, J. Endres, P. Schmitz, M. F. Zaeh, and H. P. Huber, "Femtosecond laser structuring of graphite anodes for improved lithium-ion batteries: Ablation characteristics and process design," *Journal of Laser Applications*, vol. 30, no. 3, 2018, doi: 10.2351/1.5040611.

[13] T. Waldmann, R.-G. Scurtu, K. Richter, and M. Wohlfahrt-Mehrens, "18650 vs. 21700 Li-ion cells – A direct comparison of electrochemical, thermal, and geometrical properties," *Journal of Power Sources*, vol. 472, 2020, doi: 10.1016/j.jpowsour.2020.228614.

[14] S. Link, C. Neef, and T. Wicke, "Trends in Automotive Battery Cell Design: A Statistical Analysis of Empirical Data," *Batteries*, vol. 9, no. 5, 2023, doi: 10.3390/batteries9050261.

[15] G. Zou, K. Chen, X. Luo, Q. Fu, and B. Wu, "Crystal structure, morphology, and electrical properties of aluminum-doped LFP materials," *Ionics*, vol. 30, no. 5, pp. 2549-2563, 2024, doi: 10.1007/s11581-024-05489-2.

[16] M. Mangang, H. J. Seifert, and W. Pfleging, "Influence of laser pulse duration on the electrochemical performance of laser structured LiFePO4 composite electrodes," *Journal of Power Sources*, vol. 304, pp. 24-32, 2016, doi: 10.1016/j.jpowsour.2015.10.086.

[17] M. Trenn *et al.*, "Efficiency enhancement of Li-ion battery electrode structuring by pulse burst processing: results of an automated study," presented at the Laser-based Micro- and Nanoprocessing XVIII, 2024.

[18] A. H. A. Lutey, A. Fortunato, A. Ascari, S. Carmignato, and C. Leone, "Laser cutting of lithium iron phosphate battery electrodes: Characterization of process efficiency and quality," *Optics & Laser Technology*, vol. 65, pp. 164-174, 2015, doi: 10.1016/j.optlastec.2014.07.023.

[19] Y. Sterzl and W. Pfleging, "Extending the 3D-battery concept: large areal ultrashort pulsed laser structuring of multilayered electrode coatings," *Proc. of SPIE*, vol. 12409, p. 9, 2023, doi: 10.1117/12.2650288.

[20] A. Meyer, Y. Sterzl, and W. Pfleging, "High repetition ultrafast laser ablation of graphite and silicon/graphite composite electrodes for lithium-ion batteries," *Journal of Laser Applications*, vol. 35, no. 4, 2023, doi: 10.2351/7.0001180.

[21] J. Kriegler *et al.*, "Enhanced performance and lifetime of lithium-ion batteries by laser structuring of graphite anodes," *Applied Energy*, vol. 303, 2021, doi: 10.1016/j.apenergy.2021.117693.

[22] P. Zhu, B. Ebert, P. Smyrek, and W. Pfleging, "The Impact of Structural Pattern Types on the Electrochemical Performance of Ultra-Thick NMC 622 Electrodes for Lithium-Ion Batteries," *Batteries*, vol. 10, no. 2, 2024, doi: 10.3390/batteries10020058.